10

Interaction of wrinkles and folds of a graphene sheet lying on a flat substrate

© A.V. Savin[1,2], O.I. Savina[2]

[1] N.N. Semenov Federal Research Center of Chemical Physics, Russian Academy of Sciences, Moscow, Russia
[2] Plekhanov Russian University of Economic, Moscow, Russia

E-mail: asavin00@gmail.com, asavin@chph.ras.ru

Received February 9, 2024
Revised February 9, 2024
Accepted February 19, 2024

The interaction of wrinkles and vertical folds in single-layer and multilayer graphene sheets lying on a flat substrate was simulated. It is shown that when the sheet slides freely on the substrate, the interaction of wrinkles and folds is reduced to tugging of the part of the sheet located between them. The interaction of two wrinkles always leads to the growth of the larger one due to the disappearance of the smaller one, and the interaction of a fold with a wrinkle always leads to an increase in the first and the disappearance of the second. The interaction of two folds can only lead to a change in their shape. Therefore, with low uniaxial compression, only one wrinkle can form in the sheet, and with strong uniaxial compression, only several stable folds can form. The pinning of sheet atoms on the substrate can lead to the existence of several stable wrinkles. Depinning the sheet at high temperatures leads to the disappearance of wrinkles and the formation of vertical folds from them. This scenario explains the mechanism of action of thermal annealing of small wrinkles in graphene.

Keywords: graphene, graphene wrinkles and folds, flat substrate.

DOI: 10.61011/PSS.2024.04.58206.22

1. Introduction

Carbon atoms can create numerous structures, of which the monatomic crystalline layer — graphene has recently attracted much attention from researchers [1–5]. This nanomaterial raises interest because of its unique electronic [6], mechanical [7] and thermal properties [8,9].

A popular method for producing graphene is the chemical vapor-phase deposition (CVD) method, in which graphene is grown on a substrate in a carbon-rich environment. The CVD method often results in the occurrence of topological defects (during the cooling the graphene sheet undergoes an out-of-plane deformation bending), such as ripples [10] and wrinkles [11]. Defects of this type can be formed because of the roughness of the substrate [12] and because of the different thermal expansion of graphene and the substrate [13]. The presence of such defects can change the properties of graphene: electrical conductivity [11], thermal conductivity [14,15], elasticity [16]. The wrinkle and fold structures formed on the sheet can be used as channels for the injection and storage of liquid between graphene and its substrate [17], as well as for its spatially selective chemical functionalization [18]. For this reason the understanding the laws of wrinkle and crease formation and explaining the mechanisms of their interactions is important for creating graphene-based nanodevices.

Out-of-plane (transverse) deformations of graphene can be divided into ripples (corrugations), wrinkles and crumpling (folds) depending on their physical dimensions and topology [19,20]. Quasi-analytical models based on variations calculus [11,21–26], models based on continuum mechanics using the finite element method [27,28] and full-atomic models using molecular dynamics were used for describing individual wrinkles and folds [29–31].

A two-dimensional chain model describing the longitudinal section of the nano-ribbon was recently proposed to describe the dynamics of wrinkles and folds of graphene nano-ribbon lying on a flat substrate [32]. The purpose of this study is to use this model for explaining the mechanisms of interaction of wrinkles and folds in single-layer and multilayer graphene sheets lying on a flat substrate.

2. 2D model of a multilayer graphene sheet on a flat substrate

It is convenient to use a two-dimensional molecular chain model for describing a multilayer graphene sheet which allows describing uniaxial deformations of the sheet with high accuracy. Longitudinal and bending transversely isotropic oscillations of a sheet can be described using only the dynamics of a molecular chain, which constitutes a linear section of the sheet. Such a 2D model of the chain describing the longitudinal and bending movements of the nano-ribbon is presented in Ref. [33,34]. This model was used to describe the wrinkles and folds of a single-layer graphene sheet on a flat substrate [32].

A scheme for construction of a chain model of a multilayer graphene sheet lying on a flat substrate is shown in Figure 1. The model of a single-layer graphene sheet lying in a plane parallel to the plane xy, with a zigzag structure along the axis x describes a cross section of the sheet in which all atoms with the same coordinate x correspond to one particle. All these atoms move synchronously in case of transversely isotropic oscillations, changing only the coordinates xz, but without changing the coordinate y. In this case, the Hamiltonian of the sheet can be written as the 2D chain

$$H = \sum_n \left[\frac{1}{2} M(\dot{\mathbf{u}}_n, \dot{\mathbf{u}}_n) + V(r_n) + U(\theta_n) + Z(\mathbf{u}_n) + \frac{1}{2} \sum_{|k-n|>5} W(r_{n,k}) \right], \quad (1)$$

where the two-dimensional vector $\mathbf{u}_n = (x_n, z_n)$ sets the coordinates of n-th particle of the chain with a mass of $M = 12m_p$ ($m_p = 1.66 \cdot 10^{-27}$ kg — proton mass).

The potential

$$V(r) = \frac{1}{2} K_x (r - a)^2 \quad (2)$$

describes the longitudinal stiffness of the chain, K_x — the stiffness of the interaction, a — the equilibrium length of the bond (chain pitch), $r_n = |\mathbf{u}_{n+1} - \mathbf{u}_n|$ — the distance between adjacent nodes n and $n + 1$.

The potential

$$U(\theta) = \varepsilon_1 [1 + \cos(\theta)] \quad (3)$$

describes the bending stiffness of the chain, θ — the angle between two adjacent bonds, $\cos(\theta_n) = -(\boldsymbol{\nu}_{n-1}, \boldsymbol{\nu}_n)/r_{n-1} r_n$, vector $\boldsymbol{\nu}_n = \mathbf{u}_{n+1} - \mathbf{u}_n$.

The potential $W(r_{n,k})$ describes weak non-valent interactions of remote nodes of the chain n and k, $r_{n,k} = |\mathbf{u}_n - \mathbf{u}_k|$ — the distance between nodes. These interactions can be described with high accuracy by the Lennard–Jones potential (5,11)

$$W(r) = \varepsilon_2 [5(r_0/r)^{11} - 11(r_0/r)^5]/6, \quad (4)$$

with equilibrium length $r_0 = 3.607$ Å and interaction energy $\varepsilon_2 = 0.00832$ eV [32].

The parameters of potentials (2), (3) are determined in [33,34] from the analysis of dispersion curves of the graphene nano-ribbon: longitudinal stiffness $K_x = 405$ N/m, chain pitch $a = r_{CC}\sqrt{3}/2 = 1.228$ Å ($r_{CC} = 1.418$ Å — valence bond length C–C in graphene sheet), energy $\varepsilon_1 = 3.5$ eV.

The potential $Z(\mathbf{u})$ describes the interaction of the nodes of the chain (atoms of the sheet) with the flat substrate on which it lies. The energy of the interaction of the atom with a half-space $z \le 0$ is described by the Lennard–Jones

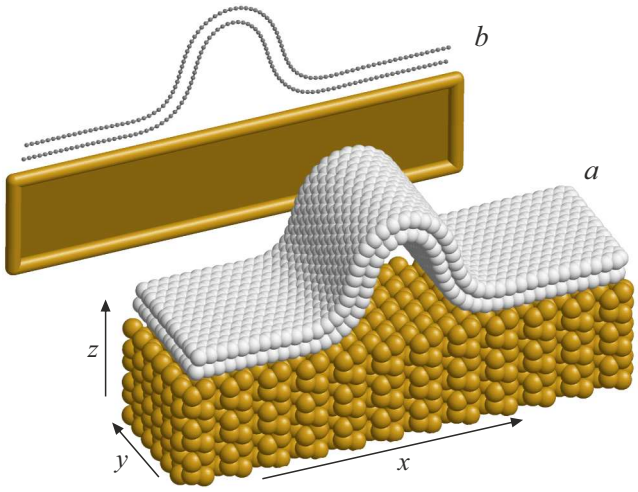

Figure 1. The scheme of construction of a two-dimensional chain model for modeling wrinkles and folds of a multilayer graphene sheet on a flat silicon oxide substrate SiO_2: (a) a full-atomic wrinkle model of a two-layer graphene lying on a flat crystal surface SiO_2, (b) a two-dimensional chain model of a two-layer sheet lying on a flat substrate.

potential (3, 9) [27,28,35]:

$$Z(\mathbf{u}) = Z(z) = \varepsilon_0 [(h_0/z)^9 - 3(h_0/z)^3]/2, \quad (5)$$

where ε_0 — the interaction energy (adhesion energy), h_0 — the equilibrium distance to the surface of the half-space. For a silicon oxide substrate SiO_2 energy $\varepsilon_0 = 0.074$ eV, distance $h_0 = 5$ Å [36].

The Hamiltonian of the K-layer sheet will have the following form

$$H = \sum_{j=1}^{K} \sum_{n=1}^{N} \frac{1}{2} M(\dot{\mathbf{u}}_{n,j}, \dot{\mathbf{u}}_{n,j}) + E, \quad (6)$$

where N — the number of nodes in each chain, $\mathbf{u}_{n,j} = (x_{n,j}, z_{n,j})$ — the vector specifying the positions of n-th node of the j-th chain (of the j-th layer). Potential energy of a multilayer structure

$$E = \sum_{j=1}^{K} \sum_{n=1}^{N} \left[V(r_{n,j}) + U(\theta_{n,j}) + \frac{1}{2} \sum_{|k-n|>5} W(r_{n,j;k,j}) \right] + \sum_{j=1}^{K-1} \sum_{i=j+1}^{K} \sum_{n=1}^{N} \sum_{l=1}^{N} W(r_{n,j;l,i}) + \sum_{j=1}^{K} \sum_{n=1}^{N} Z(\mathbf{u}_{n,j}), \quad (7)$$

where the first sum describes the deformation energy of all chains (all layers of the sheet), the second sum describes the energy of interchain interaction (interaction of layers), the third sum describes the energy of interaction of layers of the sheet with a flat substrate $z = 0$. Here the distance $r_{n,j} = |\boldsymbol{\nu}_{n,j}|$, the vector $\boldsymbol{\nu}_{n,j} = \mathbf{u}_{n+1,j} - \mathbf{u}_{n,j}$, the angle $\theta_{n,j}$ is determined us-

ing the equation $\cos(\theta_{n,j}) = -(\boldsymbol{\nu}_{n-1,j}, \boldsymbol{\nu}_{n,j})/r_{n-1,j}r_{n,j}$, distance $r_{n,j;l,i} = |\mathbf{u}_{n,j} - \mathbf{u}_{l,i}|$.

It should be noted that the Hamiltonians of the chain (1) and (6) give the deformation energy of the nanoribbon, which falls on the longitudinal ban of the width $\Delta y = \sqrt{3}r_{CC}$.

3. The stationary states of a uniaxially compressed graphene sheet

It is necessary to solve the problem of the minimum potential energy of a multilayer chain with periodic boundary conditions for finding the stationary states of a uniaxially compressed graphene sheet

$$E \to \min: \quad \{\mathbf{u}_{n,j}\}_{n=1,j=1}^{N,K} \tag{8}$$

at a period value of $L = (1-d)Na$, where N — the number of chain links, $d < 1$ — the chain compression ratio (chain compression as a percentage $p = d \cdot 100\%$).

The problem (8) was solved numerically by the conjugate gradient method, using chains of $N = 300$, 600, 1000 links. The solution of the problem showed that the following three basic states of a longitudinally compressed chain are possible: a uniformly compressed flat state, a state with a localized convex wrinkle (with a bubble-like empty area between the sheet and substrate) — see Figure 2, *a–c* and the state with the vertical fold of the sheet — see Figure 2, *d–i*.

Let $\{\mathbf{u}_{n,k}\}_{n=1,j=1}^{N,K}$ is the solution of the minimum energy problem (8) (stationary state of a longitudinally compressed graphene sheet on a flat substrate). The state will be characterized by the energy E, tension of the chain in a weakly deformed straight region of the chain

$$F = \sum_{j=1}^{K} V'(r_{n,j}) + \frac{1}{2}\sum_{k=n+6}^{n+50} W'(r_{n,j;k,j}) + \sum_{i=1,i\neq j}^{K}\sum_{k=n}^{n+50} W'(r_{n,j;k,i})(x_{k,i} - x_{n,j})/r_{n,j;k,i} \tag{9}$$

and amplitude

$$A = \max_{n}(z_{n,K}) - \sum_{n=1}^{20}(z_{n,K} + z_{N+1-n,K})/40.$$

The tension of the chain (9) in a straight section does not depend on the node number n. It is sufficient to determine the tension F for $n = 1$ if the deformation of the chain is concentrated in its center. The amplitude A for a wrinkle or fold is found as the maximum deviation from the equilibrium value of the transverse coordinate of the upper sheet (chains with $j = K$). For a uniformly compressed linear state $A = 0$.

The dependence of the energy E, tension F and amplitude of the transverse displacement A on the compression ratio of the sheet d is shown in Figure 3. The numerical solution of the problem (8) showed that the homogeneously compressed flat state of the sheet is stable at $d \le d_0$, where the critical value is $d_0 > 0$. Hooke's law holds when a flat sheet is homogeneously compressed (stretched) ($A \equiv 0$): energy $E \propto d^2$, tension $F \propto d$ — see curves *1*.

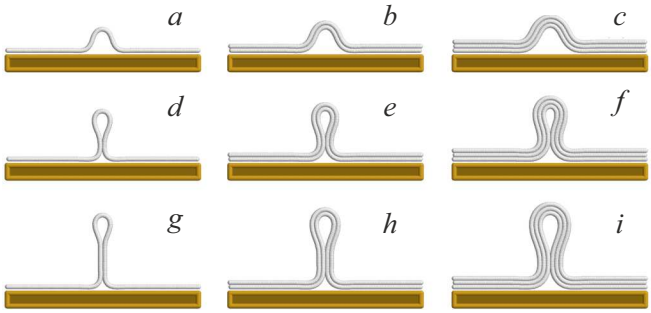

Figure 2. The type of wrinkle for (a) single-layer, (b) two-layer, (c) three-layer graphene sheet lying on a flat silicon oxide substrate (compression $d = 0.05$, $N = 300$). The type of fold for a single-layer, double-layer, three-layer sheet with $d = 0.20$ (d), (e), (f) and $d = 0.30$ (g), (h), (i).

Wrinkles with an empty inner cavity exist with compression $d_{w,1} \le d \le d_{w,2}$, where the minimum value is $d_{w,1} \in (0, d_0)$. The energy E and the amplitude A monotonously increase with an increase of compression and the tension F monotonously decreases — see curves *2, 4, 6*. The decrease of F is attributable to the increase of amplitude, the part of the surface of the „bubble" adjacent to the substrate monotonously decreases. The interaction of this part of the sheet with the substrate causes tension in the rest of the chain (this tesion prevents the chain from lying completely on the substrate).

An increase of the chain compression results in the collapse of wrinkles — they fold forming a fold with a dense narrow multilayer leg with a drop-shaped head — see Figure 2, *d–i*. Vertical folds exist with the compression $d \ge d_f$, where the minimum value is $d_f \in (d_0, d_{w,2})$.

The critical value of compression $d_0, d_{w,1}, d_{w,2}, d_f$, for K-layered sheets are given in the table. The value d_0 does not depend on the length of the chain. The width of the wrinkle interval $d_{w,2} - d_{w,1}$ and the value d_f monotonously decrease with an increase of the number of chain links N.

The energy and amplitude of the fold grow as linear functions with an increase of d: $E \propto d$, $A \propto d$; and the residual tension in the chain monotonously tends to a constant value: $F \to F_0 > 0$, for $d \to 1$ — see curves *3, 5, 7*. The reason is that the growth of the fold in case of compression of the chain is attributable to the increase of the length of its leg, while the shape of the part of the leg adjacent to the substrate practically does not change — see Figure 2, *d–i*. It should be noted that the residual tension in a chain with a fold is always less than the tension in a chain with a wrinkle.

The critical compression values d_0, $d_{w,1}$, $d_{w,2}$, d_f for K-layered chain (for K-layered sheet) of N links

N		300			600			1000		
K	d_0	$d_{w,1}$	$d_{w,2}$	d_f	$d_{w,1}$	$d_{w,2}$	d_f	$d_{w,1}$	$d_{w,2}$	d_f
1	0.035	0.017	0.136	0.094	0.013	0.068	0.050	0.011	0.041	0.033
2	0.026	0.014	0.163	0.109	0.011	0.082	0.057	0.009	0.049	0.037
3	0.021	0.013	0.191	0.125	0.010	0.096	0.065	0.008	0.068	0.039

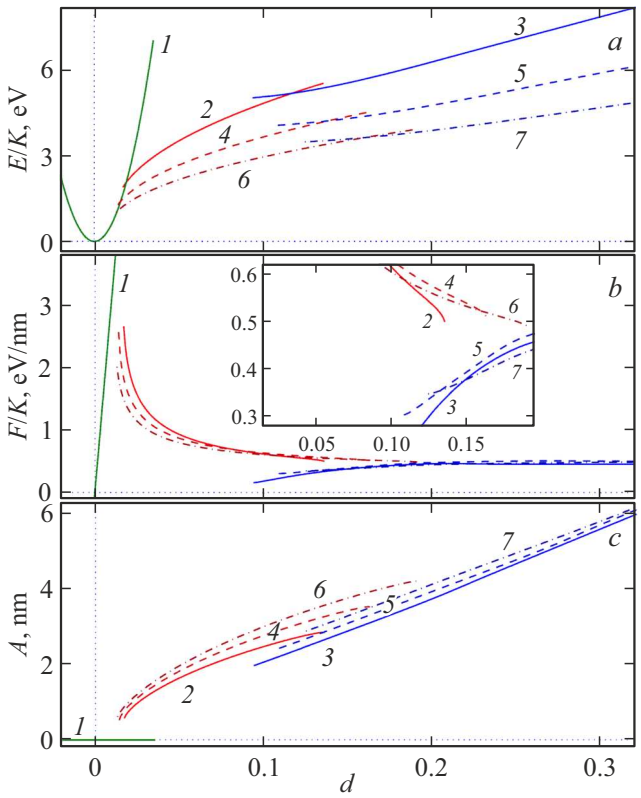

Figure 3. The dependence (a) of energy E, (b) of tension F, (c) of amplitude of transverse displacements A from compression ratio d of a multilayer cyclic chain of $N = 300$ links. Curves *1* — for longitudinal uniform compression; curves *2, 4, 6* — for a wrinkle of K-layered sheet ($K = 1, 2, 3$); curves *3, 5, 7* — for the fold of K-layered sheet ($K = 1, 2, 3$).

4. Interaction of wrinkles and folds

The dependence of the residual tension F on the degree of compression of the chain d (monotonous decrease for wrinkles and growth for folds with increase of d — see Figure 3, b) allows making a conclusion that if two wrinkles are present in a compressed cyclic chain, then the larger one will grow because of the decrease of the small one. Each wrinkle will exert pressure (force F) on the part of the chain adjacent to the substrate. If a wrinkle exerts less pressure, then as a result of the addition of pressures directed against each other, it will begin to draw in a chain, increasing its own amplitude and reducing the amplitude of the other wrinkle. The fold always exerts a weaker pressure than the wrinkle, so it will always pull the chain into itself until the wrinkle disappears.

The interaction of wrinkles and folds is reduced to the pulling of a part of the chain located between them. Therefore, wrinkles and folds can interact over long distances if the chain can freely slide over the substrate. The interaction of a pair of wrinkles should result in the growth of a larger wrinkle due to the disappearance of a smaller one, and the interaction of a fold with a wrinkle should always result in the growth of the former one due to the disappearance of the latter one.

Let's conduct a numerical simulation of the interaction of wrinkles and folds. Let's take two stationary states of a cyclic chain of $N = 300$ links with different compression values d_1 and d_2 for this purpose. Let's combine these two chains into one cyclic chain of $2N$ links with a period (length) of $L = (2-d_1-d_2)aN$. The first half of the chain will correspond to deformations of the chain with compression d_1, the second half of the chain will correspond to deformations of the chain with compression d_2. Compression of the combined chain $d = (d_1 + d_2)/2$.

Let's simulate the dynamics of the combined chain. Let's numerically integrate the system of equations of motion corresponding to the Hamiltonian (6) for this purpose:

$$M\ddot{\mathbf{u}}_{n,j} = -\frac{\partial H}{\partial \mathbf{u}_{n,j}}, \quad n = 1, \ldots, 2N, \quad j = 1, \ldots, K, \quad (10)$$

with the initial condition

$$\{x_{n,j}(0) = x_{n,j,1},\, z_{n,j}(0) = z_{n,j,1}\}_{n=1,\,j=1}^{N,K},$$

$$\{x_{n,j}(0) = N(1-d_1)a + x_{n-N,j,2},\, z_{n,j}(0) = z_{n-N,j,2}\}_{n=N+1,\,j=1}^{2N,K},$$

$$\{\dot{x}_{n,j}(0) = 0,\, \dot{z}_{n,j}(0) = 0\}_{n=1,\,j=1}^{2N,K}, \quad (11)$$

where $\{x_{n,j,i}, z_{n,j,i}\}_{n=1,\,j=1}^{N,K}$ is the solution of the problem (8) with compression $d = d_i$, $i = 1, 2$.

Numerical integration of the system of equations of motion (10) with the initial condition (11) showed that the interaction of two wrinkles always results in the growth of a wrinkle with the largest amplitude because of the disappearance of a wrinkle with a smaller amplitude — see Figure 4, a and 5, a. For instance, only one wrinkle corresponding to the compression of the combined chain

$d = 0.055$ remains in the chain for a single-layer sheet at $d_1 = 0.06$, $d_2 = 0.05$, as a result of interaction. The interaction of wrinkles also results in the disappearance of the second wrinkle for a three-layer sheet at $d_1 = 0.20$, $d_2 = 0.10$ — only one wrinkle remains in the chain, the growth of which results in its transition to a fold.

The interaction of the fold with the wrinkle always results in an increase of the fold because of the disappearance of the wrinkle — see Figure 4, *b* and 5, *b*. The interaction of the two folds results only in a periodic change in their shape due to the pulling of chains. Therefore, it can be concluded that the compression of a single-layer and multi-layer sheet can only result in the formation of one wrinkle at $d < d_f$ and in the formation of several folds at $d > d_f$. We will simulate the dynamics of a uniformly compressed chain at different compression values to verify this.

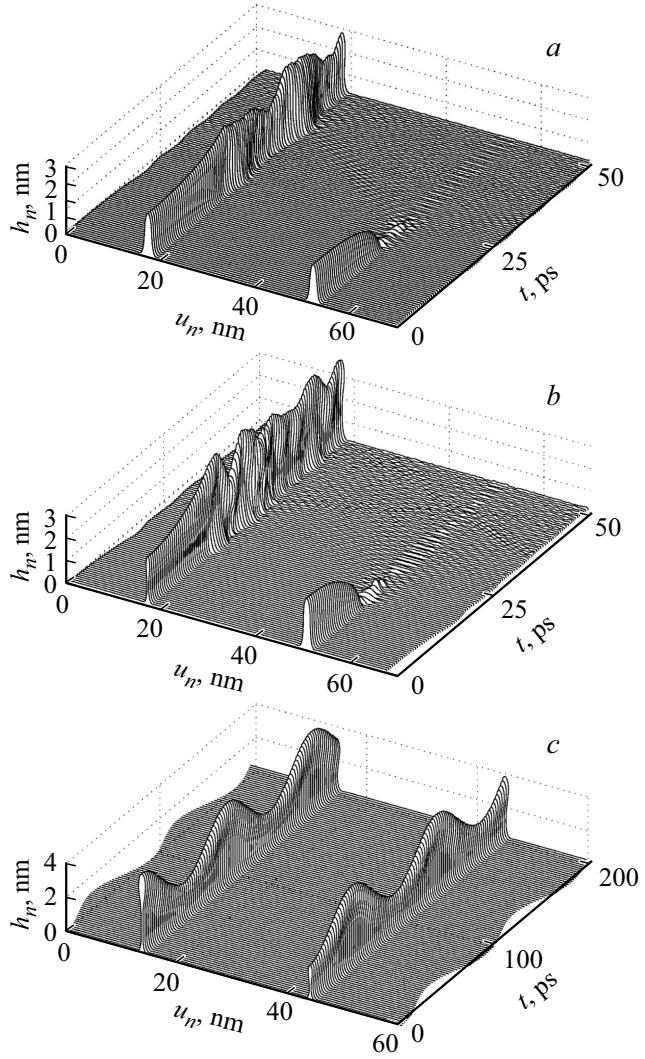

Figure 4. Interaction: (*a*) wrinkles corresponding to compression $d_1 = 0.06$, $d_2 = 0.05$; (*b*) folds and wrinkles with $d_1 = 0.08$ and $d_2 = 0.06$; (*c*) two folds with compression $d_1 = 0.10$ and $d_2 = 0.08$ chains of $N = 300$ links. The number of sheet layers is $K = 1$. The dependence on time t of the shape of the first layer $\{u_n = x_{n,1},\, h_n = z_{n,1} - h_0\}_{n=1}^{600}$ is shown.

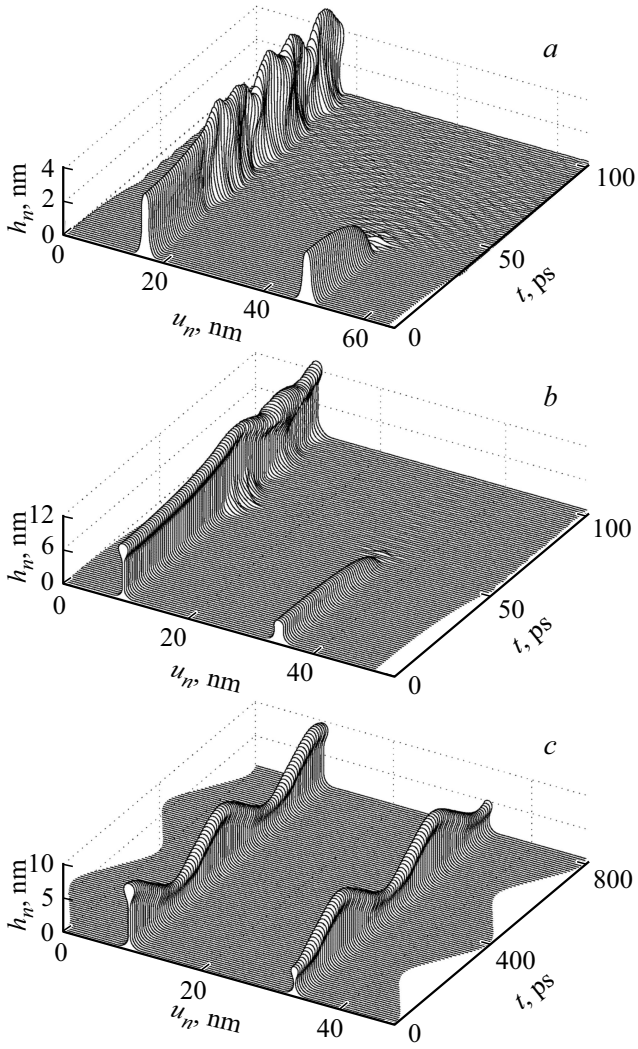

Figure 5. Interaction: (*a*) wrinkles corresponding to compression $d_1 = 0.15$, $d_2 = 0.10$; (*b*) folds and wrinkles with $d_1 = 0.50$ and $d_2 = 0.15$; (*c*) two folds with compression $d_1 = 0.50$ and $d_2 = 0.20$ chains of $N = 300$ links. The number of sheet layers is $K = 3$. The dependence on time t of the shape of the first layer $\{u_n = x_{n,1},\, h_n = z_{n,1} - h_0\}_{n=1}^{600}$ is shown.

5. The formation of wrinkles and folds in case of compression of the chain

Let's take a homogeneously compressed cyclic chain of $N = 1000$ links to simulate the formation of wrinkles and folds. Let's put it in a Langevin thermostat and consider its further dynamics. Let's numerically integrate the system of Langevin equations for this purpose

$$\left\{ M\ddot{\mathbf{u}}_{n,j} = -\frac{\partial H}{\partial \mathbf{u}_{n,j}} - \Gamma M\dot{\mathbf{u}}_{n,j} - \Xi_{n,j} \right\}_{n=1,\,j=1}^{N,K}, \qquad (12)$$

where $\Gamma = 1/t_r$ — the coefficient of friction (thermostat relaxation time $t_r = 2\,\text{ps}$), $\Xi_{n,j} = (\xi_{n,j;1}, \xi_{n,j;2})$ — a two-dimensional vector of normally distributed random

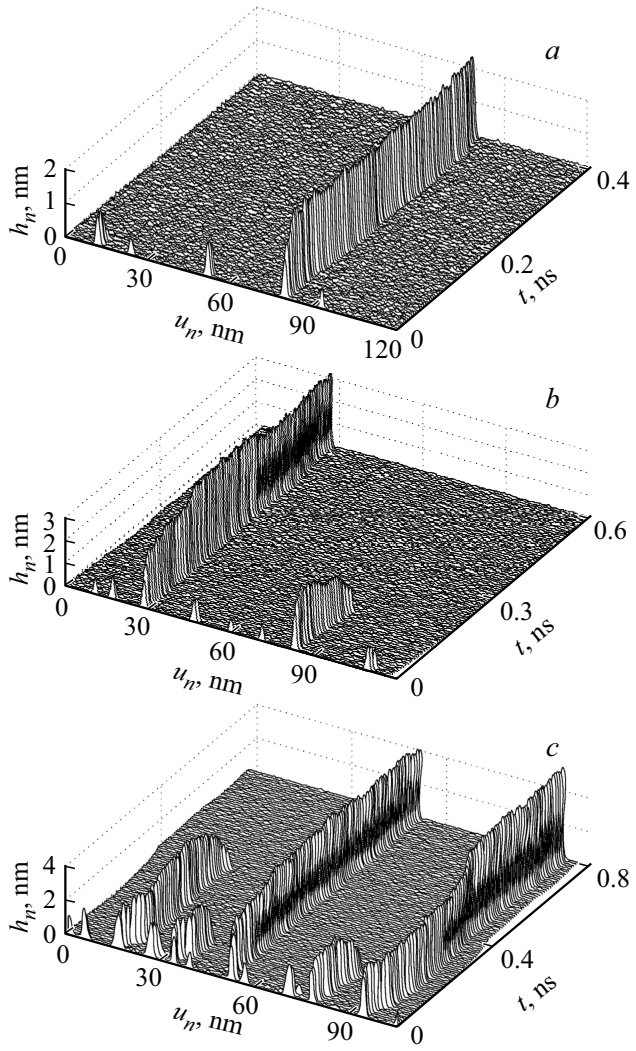

Figure 6. The formation of one wrinkle with compression $d = 0.025$, (b) one fold at $d = 0.05$ and (c) of two folds at $d = 0.25$ in a uniformly compressed two-layer graphene sheet (a). Number of links $N = 1000$, number of layers $K = 2$, temperature $T = 300$ K. The dependence of the shape of the first layer on time t is shown: $\{u_n = x_{n,1}, h_n = z_{n,1} - h_0\}_{n=1}^{N}$.

Langevin forces with correlation functions

$$\langle \xi_{n,j_1;i_1}(t_1)\xi_{k,j_2;i_2}(t_2)\rangle = 2Mk_{\mathrm{B}}T\Gamma\delta_{nk}\delta_{j_1j_2}\delta_{i_1i_2}\delta(t_1 - t_2)$$

(k_{B} — Boltzmann constant, T — thermostat temperature).

Let's take a homogeneously compressed stationary state of the chain as the initial condition of the system of equations (12)

$$\{x_{n,j}(0) = (n-1)(1-d)a + b_j,$$
$$z_{n,j}(0) = h_0 + (j-1)h_1,$$
$$\dot{x}_{n,j}(0) = 0, \quad \dot{z}_{n,j}(0) = 0\}_{n=1,j+1}^{N,K}, \qquad (13)$$

where $b_j = 0$ for odd j, $b_j = a/2$ for even j, $h_1 = 3.33$ Å [chain length $L = (1-d)Na$]. The presence of a thermostat allows removing the excess energy of the initial homogeneous compression from the chain. Let's take the temperature of the thermostat of $T = 300$ K.

Numerical integration of the Langevin equation system (12) with the initial condition (13) showed that only one wrinkle can form in the sheet with the compression $d < d_f$ — see Figure 6, a. Several wrinkles are first formed in the system in case of compression $d = 0.05 > d_f$, one of which absorbs all the others and then it forms a vertical fold — see Figure 6, b. Several growing wrinkles are formed first in case of a stronger compression $d = 0.15$, two of which form vertical folds, and the rest disappear. The folds form stable states — see Figure 6, a. The scenario of the formation of wrinkles and folds remains the same for single-layer, double-layer, three-layer sheets and is fully consistent with the results of modeling of their interaction.

6. Thermal annealing of wrinkles

The above results are valid only if the chain (sheet) can slide freely over the substrate. The wrinkles and folds of the sheet will interact only over short distances if the interaction with the substrate prevents such sliding, if the chain nodes are pinned on the substrate grid. In this case, several wrinkles may exist in the chain at the same time, forming stable structures in this chain.

Let's describe the interaction of the chain nodes with the substrate with a periodic potential of x for describing the pinning effect

$$Z(u) = \left[\frac{1}{2}\varepsilon_0 - \frac{1}{4}\varepsilon_p\left(1 - \cos\frac{2\pi x}{a}\right)\right]\left\{\left(\frac{h_0}{z}\right)^9 - 3\left(\frac{h_0}{z}\right)^3\right\}, \qquad (14)$$

where $\varepsilon_p \geq 0$ — the height of the energy periodic relief along the substrate (pinning energy). The potential (14) coincides with potential (5) in the absence of pinning, at $\varepsilon_p = 0$.

Let's take the characteristic value of the pinning energy $\varepsilon_p = 0.003$ eV. The solution of the problem (8) in case of use of the potential of interaction with the substrate (14) shows that a stable system of non-interacting wrinkles can already exist in the compressed chain. For instance, there is a stable system of 8 wrinkles in a single-layer chain ($K = 1$) of $N = 1000$ links with compression $d = 0.1$. Let's consider the behavior of this system at different temperatures.

The numerical integration of the Langevin equation system (12) showed that the system of non-interacting wrinkles is present at low temperatures. Thermally activated chain depinning begins with an increase of the temperature as a result of which it becomes possible for the chain to temporarily slide along the substrate. Therefore, the wrinkles begin to interact over greater distances. The dynamics of the chain at different temperatures is shown in Figure 7. For instance, all wrinkles remain in the chain at $T = 100$ K. Two wrinkles disappear at $T = 200$ they are absorbed by their larger neighbors and 6 wrinkles remain in the chain. 5 wrinkles remain in the chain at $T = 300$ K.

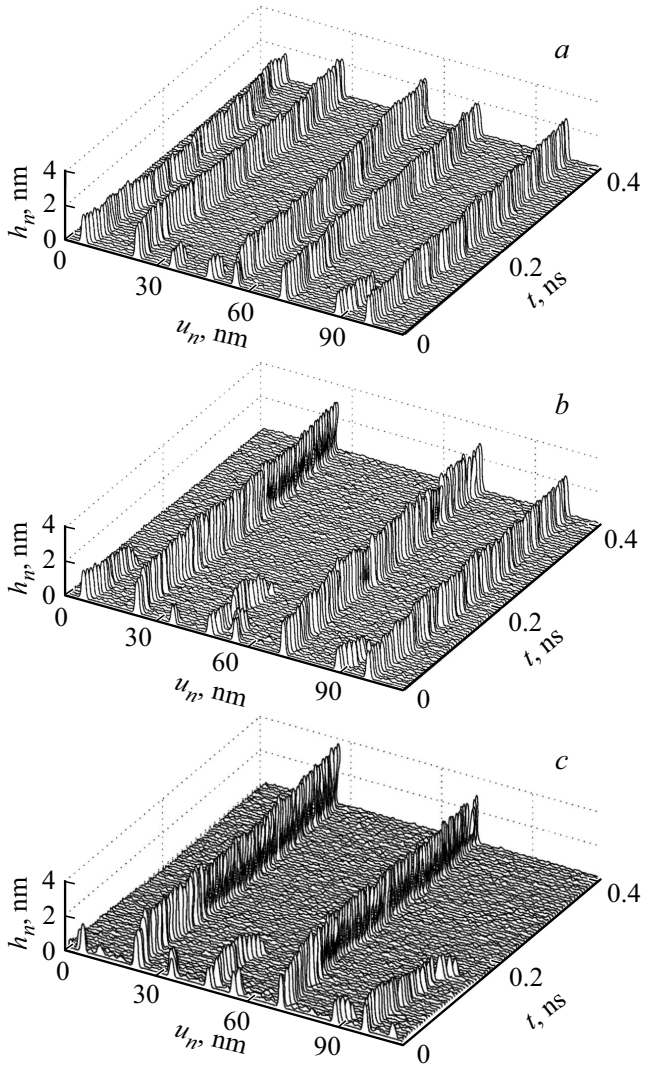

Figure 7. Dynamics of wrinkles and folds in a compressed single-layer graphene sheet (compression $d = 0.1$) in the presence of attachment to the substrate (pinning energy $\varepsilon_p = 0.003\,\text{eV}$) at temperature (*a*) $T = 300$, (*b*) $T = 400$ and (*c*) $T = 500\,\text{K}$. The number of links $N = 1000$, the number of layers $K = 1$. The dependence of the shape of the first layer on time t is shown: $\{u_n = x_{n,1}, h_n = z_{n,1} - h_0\}_{n=1}^{N}$.

Two stable wrinkles and one fold remain in the chain at $T = 400\,\text{K}$. The chain is completely depinned at high temperature $T = 500\,\text{K}$, it begins to slide almost freely on the substrate. All wrinkles disappear as a result, and a stable system of two folds remains in the sheet. Wrinkles have similar dynamics in case of two and three-layer sheets.

The simulation explains the mechanism of elimination of small wrinkles in case of thermal annealing [37]. Annealing at a temperature of $T = 200^\circ\text{C}\,(473\,\text{K})$ of a graphene sheet lying on a substrate SiO_2 result in the disappearance of wrinkles with an amplitude of $A = 1.5\,\text{nm}$, and wrinkles with $A \geq 1.5\,\text{nm}$ remain stable. Our simulation shows that annealing here results in thermally activated depinning of the graphene sheet from the substrate. As a result, all wrinkles with small amplitudes disappear, and large wrinkles grow and turn into vertically standing stable folds.

7. Conclusion

The interaction of wrinkles and vertical folds in single-layer and multilayer graphene sheets lying on a flat substrate (on the flat surface of a silicon oxide crystal SiO_2) was simulated using a two-dimensional chain model describing the longitudinal section of a graphene nano-ribbon. Uniaxial compression of such a sheet results in the formation of a localized convex wrinkle with an empty bubble-like area between the sheet and the substrate. The wrinkles fold (collapse) when the amplitude of $A \approx 2\,\text{nm}$ is reached and form vertically standing folds with dense multilayer legs and drop-shaped heads.

It was shown that the interaction of wrinkles and folds is reduced to pulling of the part of the sheet located between them when the sheet slides freely over the substrate. Such interaction can occur over long distances. The interaction of two wrinkles always results in the growth of the larger one because of the disappearance of the smaller one, and the interaction of the fold with the wrinkle results in the growth of the former one because of the disappearance of the latter one. The interaction of the two folds only results in a change of their shape. Therefore, only one wrinkle can be formed in a uniaxially compressed graphene sheet with low compression $d < d_f$ (initially, several wrinkles are formed, but then the largest wrinkle grows because of the disappearance of the other wrinkles). Either one fold or several stable folds can be formed in the sheet in case of strong compression $d > d_f$. A system of multiple wrinkles is formed at first here, too, the largest of which grow as the result of the reduction of the neighboring ones and then collapse into vertical folds. The scenario for the formation of wrinkles and folds is the same for single-layer, double- and three-layer sheets.

The wrinkles and folds will interact only over short distances if the interaction with the substrate prevents the sheet from sliding (with the pinning of the sheet on the substrate). In this case, several wrinkles can exist simultaneously in a compressed sheet, forming stable structures in this sheet. The sheet begins to slide along the substrate at high temperatures because of thermally activated depinning and wrinkles begin to interact over long distances. As a result, all wrinkles disappear, and only vertical folds remain in the sheet. This scenario explains the mechanism of action of thermal annealing of small wrinkles of graphene [37].

Funding

The research work was funded by subsidy allocated by the N.N. Semenov Federal Research Center for Chemical Physics of Russian Academy of Sciences (task No. FFZE-2022-0009).

Joint Supercomputer Center of Russian Academy of Sciences RAS.

Conflict of interest

The authors declare that they have no conflict of interest.

References

[1] K.S. Novoselov, A.K. Geim, S.V. Morozov, D. Jiang, Y. Zhang, S.V. Dubonos, I.V. Grigorieva, A.A. Firsov. Science **306**, *5696*, 666 (2004).
[2] A.K. Geim, K.S. Novoselov. Nature Mater. **6**, *3*, 183 (2007).
[3] C. Soldano, A. Mahmood, E. Dujardin. Carbon **48**, *8*, 2127 (2010).
[4] J.A. Baimova, B. Liu, S.V. Dmitriev, K. Zhou. Phys. Status Solidi RRL **8**, *4*, 336 (2014).
[5] J.A. Baimova, E.A. Korznikova, S.V. Dmitriev, B. Liu, K. Zhou. Rev. Adv. Mater. Sci. **39**, 69 (2014).
[6] A.K. Geim. Science **324**, *5934*, 1530 (2009).
[7] C. Lee, X. Wei, J.W. Kysar, J. Hone. Science **321**, *5887*, 385 (2008).
[8] A.A. Balandin, S. Ghosh, W. Bao, I. Calizo, D. Teweldebrhan, F. Miao, C.N. Lau. Nano Lett. **8**, *3*, 902 (2008).
[9] Y. Liu, C. Hu, J. Huang, B.G. Sumpter, R. Qiao. J. Chem. Phys. **142**, *24*, 244703 (2015).
[10] L. Tapasztó, T. Dumitric, S.J. Kim, P. Nemes-Incze, C. Hwang, L.P. Biró. Nature Phys. **8**, *10*, 739 (2012).
[11] W. Zhu, T. Low, V. Perebeinos, A.A. Bol, Y. Zhu, H. Yan, J. Tersoff, P. Avouris. Nano Lett. **12**, *7*, 3431 (2012).
[12] C.H. Lui, L. Liu, K.F. Mak, G.W. Flynn, T.F. Heinz. Nature **462**, *7271*, 339 (2009).
[13] A.N. Obraztsov, E.A. Obraztsova, A.V. Tyurnina, A.A. Zolotukhin. Carbon **45**, *10*, 2017 (2007).
[14] S. Chen, Q. Li, Q. Zhang, Y. Qu, H. Ji, R.S. Ruoff, W. Cai. Nanotechnology **23**, *36*, 365701 (2012).
[15] C. Wang, Y. Liu, L. Li, H. Tan. Nanoscale **6**, *11*, 5703 (2014).
[16] Y. Wang, R. Yang, Z. Shi, L. Zhang, D. Shi, E. Wang, G. Zhang. ACS Nano **5**, *5*, 3645 (2011).
[17] M.G. Pastore Carbone, A.C. Manikas, I. Souli, C. Pavlou, C. Galiotis. Nature Commun. **10**, 1572 (2019).
[18] S. Deng, D. Rhee, W.-K. Lee, S. Che, B. Keisham, V. Berry, T.W. Odom. Nano Lett. **19**, *8*, 5640 (2019).
[19] S. Deng, V. Berry. Mater. Today **19**, *4*, 197 (2016).
[20] B. Deng, J. Wu, S. Zhang, Y. Qi, L. Zheng, H. Yang, J. Tang, L. Tong, J. Zhang, Z. Liu, H. Peng. Small **14**, *22*, 1800725 (2018).
[21] Y. Zhang, N. Wei, J. Zhao, Y. Gong, T. Rabczuk. J. Appl. Phys. **114**, *6*, 063511 (2013).
[22] B.J. Cox, D. Baowan, W. Bacsa, J.M. Hill. RSC Adv. **5**, *71*, 57515 (2015).
[23] J. Aljedani, M.J. Chen, B.J. Cox. Mater. Res. Express **8**, *1*, 015002 (2020).
[24] J. Aljedani, M.J. Chen, B.J. Cox. RSC Adv. **10**, *27*, 16016 (2020).
[25] B.J. Cox, T. Dyer, N. Thamwattana. Mater. Res. Express **7**, *8*, 085001 (2020).
[26] J. Aljedani, M.J. Chen, B.J Cox. Appl. Phys. A **127**, 886 (2021).
[27] K. Zhang, M. Arroyo. J. Appl. Phys. **113**, 193501 (2013).
[28] K. Zhang, M. Arroyo. J. Mech. Phys. Solids **72**, 61 (2014).
[29] T. Al-Mulla, Z. Qin, M.J. Buehler. J. Phys.: Condens. Matter **27**, 345401 (2015).
[30] W. Zhu, Y. Liu, X. Wei. JOM **72**, 3987 (2020).
[31] C. Zhao, F. Liu, X. Kong, T. Yan, F. Ding. Int. J. Smart Nano Mater. **11**, *3*, 277 (2020).
[32] A.V. Savin, E.A. Korznikova, S.V. Dmitriev.Phys. Rev. B **99**, 235411 (2019).
[33] A.V. Savin, E.A. Korznikova, S.V. Dmitriev. Phys. Rev. B **92**, 035412, (2015).
[34] A.V. Savin, E.A. Korznikova, S.V. Dmitriev. FTT **57**, *11*, 2278 (2015). (in Russian).
[35] Z.H. Aitken, R. Huang. J. Appl. Phys. **107**, 123531 (2010).
[36] S.P. Koenig, N.G. Boddeti, M.L. Dunn, J.S. Bunch. Nature Nanotech **6**, 543 (2011).
[37] F. Zheng, Q.H. Thi, L.W. Wong, Q. Deng, T.H. Ly, J. Zhao. ACS Nano **14**, 2137 (2020).

Translated by A.Akhtyamov